IEEE Access
Multidisciplinary | Rapid Review | Open Access Journal

Received April 9, 2020, accepted April 20, 2020, date of publication April 22, 2020, date of current version May 8, 2020.

Digital Object Identifier 10.1109/ACCESS.2020.2989547

Ridge Gap Waveguide Based Liquid Crystal Phase Shifter

MATTHIAS NICKEL[1], (Graduate Student Member, IEEE), ALEJANDRO JIMÉNEZ-SÁEZ[1], (Student Member, IEEE), PRANNOY AGRAWAL[1], (Graduate Student Member, IEEE), AHMED GADALLAH[2], (Member, IEEE), ANDREA MALIGNAGGI[2], CHRISTIAN SCHUSTER[1], (Student Member, IEEE), ROLAND REESE[1], (Graduate Student Member, IEEE), HENNING TESMER[1], (Graduate Student Member, IEEE), ERSIN POLAT[1], (Student Member, IEEE), DONGWEI WANG[1], PETER SCHUMACHER[1], (Graduate Student Member, IEEE), ROLF JAKOBY[1], (Member, IEEE), DIETMAR KISSINGER[3], (Senior Member, IEEE), AND HOLGER MAUNE[1], (Senior Member, IEEE)

[1]Institute of Microwave Engineering and Photonics, Technische Universität Darmstadt, 64283 Darmstadt, Germany
[2]IHP–Leibniz-Institut für innovative Mikroelektronik, Im Technologiepark 25, 15236 Frankfurt (Oder), Germany
[3]Institute of Electronic Devices and Circuits, Ulm University, 89081 Ulm, Germany

Corresponding authors: Matthias Nickel (nickel@imp.tu-darmstadt.de) and Alejandro Jiménez-Sáez (jimenez@imp.tu-darmstadt.de)

This work was supported by the German Research Foundation within the DFG Project HyPAA under Grant 320392473 and the Open Access Publication Fund of Technische Universität Darmstadt. Matthias Nickel and Alejandro Jiménez-Sáez contributed equally to this work.

ABSTRACT In this paper, the gap waveguide technology is examined for packaging liquid crystal (LC) in tunable microwave devices. For this purpose, a line based passive phase shifter is designed and implemented in a ridge gap waveguide (RGW) topology and filled with LC serving as functional material. The inherent direct current (DC) decoupling property of gap waveguides is used to utilize the waveguide surroundings as biasing electrodes for tuning the LC. The bed of nails structure of the RGW exhibits an E-field suppression of 76 dB in simulation, forming a completely shielded device. The phase shifter shows a maximum figure of merit (FoM) of 70 °/dB from 20 GHz to 30 GHz with a differential phase shift of 387° at 25 GHz. The insertion loss ranges from 3.5 dB to 5.5 dB depending on the applied biasing voltage of 0 V to 60 V.

INDEX TERMS Liquid crystals (LC's), tunable phase shifter, phased array, gap waveguide, bed of nails.

I. INTRODUCTION

Nowadays, the development in communication is already driven by mobility/portability and data rate, which will be emphasized even more by future applications such as IoT, industrial digitization, 5G or autonomous driving. For concepts like cognitive radio or high data rate wireless communication, flexible filtering in the frequency or spatial domain is required. This poses additional challenges for the radio frequency (RF) frontend design. Here, varactors and phase shifters are a key component to realize tunable filters and beamsteering antennas.

This work focuses on a line-based passive phase shifter, utilizing a functional material. These kind of phase shifters are appealing due to their ease of design: They consist only of a transmission line section combined with the functional material. They do not require additional power like active or ferrite based phase shifters [1], [2], nor complicated varactor designs like loaded line or reflection type phase shifters [3]. Other advantages are their compactness and robustness compared to electromechanical approaches [4]. Further, a continuous tuning of the phase shift is possible.

The choice for the functional material fell on LC since it provides low losses especially for frequencies above 20 GHz up to the THz range [5], which makes it a promising functional material for future communication systems operating in the millimeter wave range and above. The working principle of LC is summarized in Fig. 1c. LC, being a mesophase material at room temperature, exhibits properties of a liquid and a crystal at the same time, including birefringence. The molecules of the used nematic mixture can be considered rod shaped, whereas they exhibit no long-range spatial order but a

The associate editor coordinating the review of this manuscript and approving it for publication was Weiren Zhu.

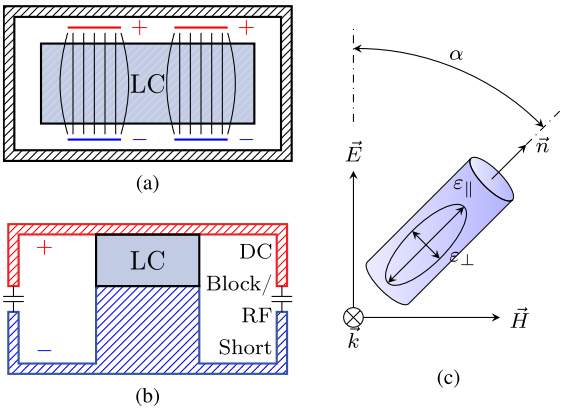

FIGURE 1. Conceptual evolution of the LC ridge gap phase shifter: (a) Cross section of a LC hollow waveguide phase shifter integrating four electrodes enabling full electric tuning of the LC. (b) A ridged hollow waveguide with DC blocks in the side walls. Here, the enclosure of the waveguide itself can act as electrodes for tuning. (c) Interaction of LC molecules with RF waves due to their birefringent property, depicted by the Fresnel ellipsoid.

certain directional order, which is macroscopically described by the director vector $\vec{n}$, see Fig. 1c. Associated with the director, the birefringent property can be described by a Fresnel ellipsoid with a permittivity $\varepsilon_\parallel$ parallel to the director and a permittivity $\varepsilon_\perp$ perpendicular to it. A transversal electromagnetic wave interacting with this kind of material will experience any permittivity on the Fresnel ellipsoid, i.e. between $\varepsilon_\perp$ and $\varepsilon_\parallel$, depending on the tilt angle α between the electric field vector $\vec{E}$ and the director $\vec{n}$. The LC molecules' orientation can be controlled in three different ways: Mechanically, utilizing surface anchoring forces, magnetically and electrically [6], where the LC will orient its molecules parallel to the field lines in order to minimize its free energy. In practical applications, usually electric tuning is used, often in combination with a mechanical pre-orientation by surface anchoring. Magnetic tuning is mostly used for material characterization and in test setups only due to its bulkiness and power consumption.

To compare the performance of different phase shifters, a figure of merit (FoM) was previously introduced [7], which relates the maximum differential phase shift achieved to the maximum insertion loss over the tuning states, described by the tuning voltage V_{bias}.

$$\text{FoM} = \frac{\max\limits_{V_{\text{bias}}} \{\Delta\Phi\}}{\max\limits_{V_{\text{bias}}} \{\text{IL}\}} \tag{1}$$

The best performance so far (FoM = 200 °/dB at $f_{\text{op}} = 30\,\text{GHz}$, [8]) is achieved with a magnetically biased hollow waveguide topology. However, for the electric tuning of liquid crystals, a biasing circuitry, i.e. electrodes are necessary to generate the quasi-static E-fields. In the case of rectangular waveguides, such electrodes need to be placed inside the waveguide, so that the DC fields can interact with the LC, see in Fig. 1. The addition of these electrodes leads to mode coupling of the TE_{10} mode into the biasing electrodes, where different kind of Stripline modes can be excited. Hence, the insertion loss is increased and the performance decreases (from FoM = 200 °/dB to FoM = 150 °/dB, [8]). To mitigate this effect, certain care has to be taken in the electrode design. For example, stepped impedance filters can be integrated into the electrodes to avoid mode coupling [9]. However, a complete suppression of these unwanted modes, especially at higher frequencies, is difficult in practice, mainly due to the small feature size close to or even beyond manufacturing tolerances.

In order to avoid these difficulties in electrode design and integration, the basic idea of this work is to utilize the waveguide surroundings itself as electrodes as depicted in Fig. 1b. For this, the waveguide is cut in half in its H-plane. In between this cut, a component has to be introduced, which serves as a short for the RF wave and as a block for the applied DC voltage. One type of waveguide, which exhibits exactly these desired properties, called gap waveguide, has been studied intensively in the last few years [10]–[14]. It consists of two parallel metal plates, where one of the plates is patterned to form a metamaterial surface, called bed of nails in this case, which prevents wave propagation in its stop band, see Fig. 2. With the help of the metamaterial pattern, an electromagnetic wave can be guided similar to a hollow waveguide but without the necessity of an electrical contact between the waveguide's side walls.

The aim of this work is to validate the applicability of the gap waveguide for a LC based phase shifter to ease the electrode integration and to improve isolation. For this, a LC filled RGW was designed and fabricated, which will be described in more detail in the next section. To ease the coupling design and to prevent tolerance issues during fabrication, this demonstrator was chosen to operate around 26 GHz

II. DESIGN AND IMPLEMENTATION

The bed of nails structure used in this work consists of periodic electric pins surrounding the desired waveguide. This structure is patterned on one of the metallic plates, acting as the bottom and side walls of the waveguide. The other plate is unpatterned, forming the top wall of the waveguide. A gap is left between the top of the nails and the top plate, so that they are DC-decoupled. Thus, the lower plate and the upper plate can act as electrodes for aligning the LC vertically. Horizontal alignment is achieved in this design by utilizing surface anchoring forces at the top and bottom plate.

The bed of nails structure realizes a high impedance surface, which limits the electromagnetic wave propagation for frequencies between 14 GHz and 37 GHz, forming an electronic band gap. For this, the designed bed of nails has to comply the following conditions [10]:

- Nail height d, corresponds to the quarter-wavelength at 22 GHz, roughly at the center of the stop-band region.

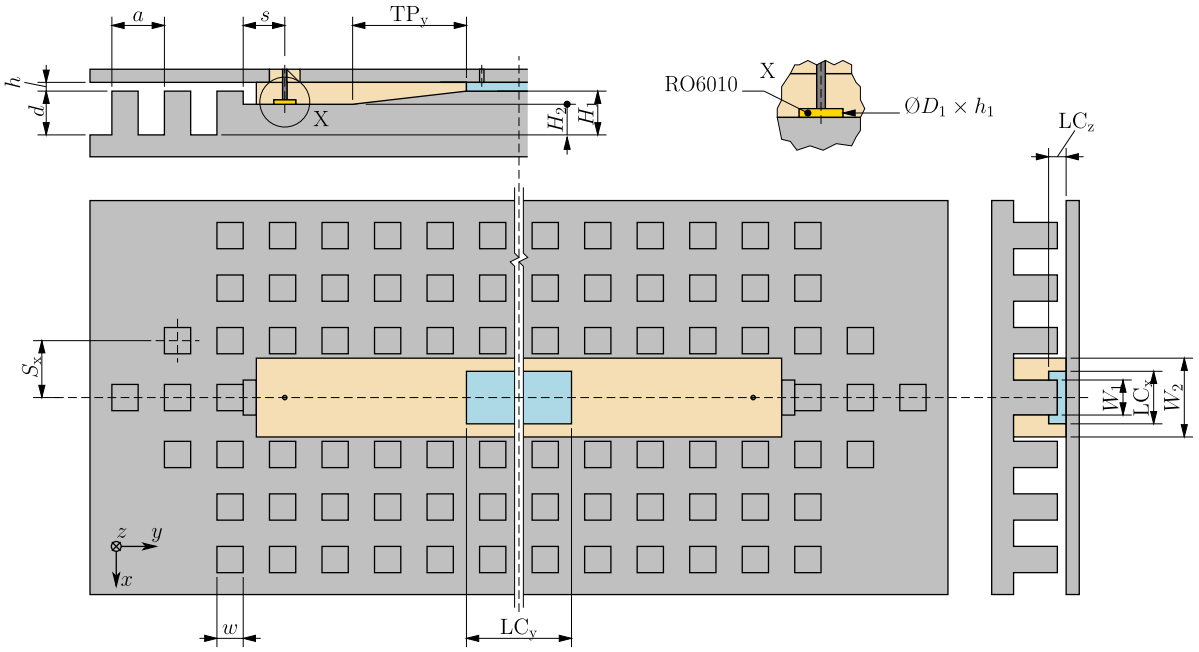

FIGURE 2. Schematic view of the RGW phase shifter including cross sections, a detailed view (X) of the capacitor section and the corresponding dimensions.

TABLE 1. Properties of the used LC mixture GT3 23001 at room temperature and $f = 19$ GHz (provided by Merck KGaA).

$\varepsilon_{r,\parallel}$	$\tan\delta_\parallel$	$\varepsilon_{r,\perp}$	$\tan\delta_\perp$	K_{11}
3.28	0.0038	2.46	0.0143	24 pN

- Space between upper and lower plate $h+d$, corresponds to the half-wavelength at 40 GHz, determining the upper end of the stop-band region.

To ensure sufficient wave guidance and shielding, three rows of nails are placed around the waveguide in a first design. However, later simulations (see Fig. 8) showed that two rows of nails are still sufficient for wave guidance and shielding, which was adapted to the final implementation in favor of fabrication simplicity and compactness.

Since the alignment speed of LC depends on field-strength and layer thickness, a ridge was introduced in the gap waveguide, reducing the distance between the lower and the upper plate to 0.2 mm for the LC section. The so designed RGW allows for the propagation of a quasi-TEM mode.

A LC container made of Rexolite is used to prevent LC-leakage. This container extends from the input to the output port as shown in Fig. 2. The length of the phase shifter part, i.e. the LC-cavity was chosen to enable a full 360° differential phase shift with the LC mixture GT3 23001 from Merck KGaA (see Table 1). This LC is filled through two holes on the upper plate, which are close to the end of the LC cavity.

Female SMA thread-in connectors are used in the top plate to connect the phase shifter to the measurement equipment. To match the impedance of the LC region (14 Ω) to the 50 Ω connectors, a linear taper reduces the ridge height. The ridge extends by $\lambda/4$ after the coax connector, where it is shorted by the first pin of the bed of nails. Moreover, the inductive nature of the connector-ridge interface is compensated by introducing a disk capacitor in Rogers RT/duroid 6010 substrate between the connector pin and the ridge (see Fig. 2). Additionally, this capacitor serves as DC block between bottom plate and SMA connector pin.

The upper plate and the lower plate are fabricated separately by milling using Brass. The Rexolite container is pressed between top and bottom plate and additionally sealed using glue. PVC alignment rings are placed around the waveguide to ensure alignment between both plates, which are then held together by Nylon screws. All separate parts except the top plate are shown in Fig. 3a. The assembled phase shifter including the top plate is depicted in Fig. 3b.

III. SIMULATIONS AND MEASUREMENTS

The phase shifter is designed and simulated using CST Studio Suite and the fabricated prototype is measured using a vector network analyzer calibrated for a frequency range of 20 GHz to 30 GHz.

For modelling the LC material inside CST Studio Suite, use is made of the tensor formula material model, which is fed by the permittivity and loss tangent tensor of the used GT3 23001 material (see Table 1). For a z-oriented LC director, the permittivity tensor is described by

$$\bar{\varepsilon} = \varepsilon_0 \begin{bmatrix} \varepsilon_{r,\perp} & 0 & 0 \\ 0 & \varepsilon_{r,\perp} & 0 \\ 0 & 0 & \varepsilon_{r,\parallel} \end{bmatrix}. \quad (2)$$

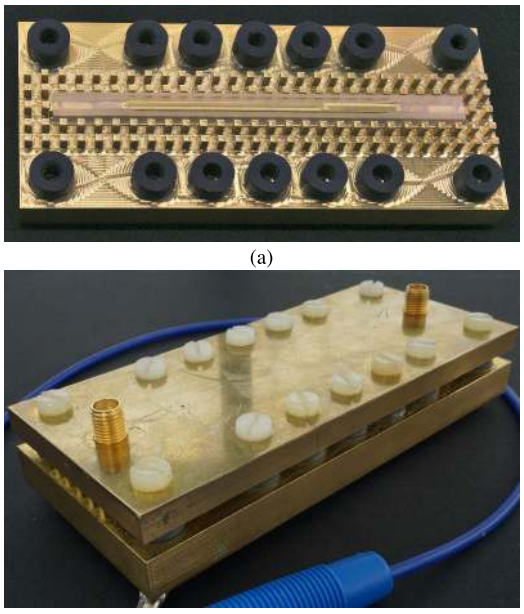

FIGURE 3. Implementation of the RGW phase shifter: (a) Bottom plate with the Rexolite container placed above the ridge and the PVC spacer rings placed in their grooves. (b) Assembled phase shifter with the top plate fixed by nylon screws. The bottom plate is connected to the blue cable for applying the bias voltage.

Arbitrary orientation of the LC director is accounted by a coordinate transformation of the microwave field components into this LC director coordinate system and back. Since wave propagation along the y-direction and LC director alignment in the xz-plane is assumed (see Fig. 2), this coordinate transformation can be carried out by rotation around the y-axis

$$\varepsilon = \mathbf{R}_{\mathrm{y}}(\alpha)\bar{\varepsilon}\mathbf{R}_{\mathrm{y}}(-\alpha), \tag{3}$$

where α is the tilt angle of the LC director with respect to the z-axis (see Fig. 1c). Hence, the final permittivity tensor formulation for the CST Studio Suite model is given by equation (6), as shown at the bottom of this page. The loss tangent tensor formulation is derived analogously.

Since there is no possibility in CST Studio Suite to simulate the LC directors orientation in dependence of the applied bias field, the model of the Freedericks cell was used to relate the bias voltage V_{bias} to the tilt angle α by [15]

$$\frac{V_{\mathrm{bias}}^2}{V_{\mathrm{th}}^2}\pi^2 \cos\alpha \sin\alpha - \frac{\partial^2\alpha}{\partial z^2} = 0, \tag{4}$$

with the threshold voltage

$$V_{\mathrm{th}} = \pi\sqrt{\frac{K_{11}}{\varepsilon_0\left(\varepsilon_{\mathrm{r},\parallel} - \varepsilon_{\mathrm{r},\perp}\right)}}, \tag{5}$$

TABLE 2. Design parameters.

Parameter	Description	Value (mm)
a	Nail period	4
w	Nail width	1.6
d	Nail height	3.4
h	Gap between top of nail and upper plate	0.2
W_1	Ridge width	2.4
W_2	Rexolite container width	6.2
H_1	Ridge height in LC cavity	3.4
H_2	Ridge height at connector interface	2.4
S_x	Ridge and first column of nail separation	4.5
$\mathrm{TP_y}$	Linear taper length	7
s	Termination stub length	2.7
$\mathrm{LC_y}$	LC cavity length	64
$\mathrm{LC_x}$	LC cavity width	4.2
$\mathrm{LC_z}$	LC cavity height	1
D_1	Disk capacitor diameter	1.5
h_1	Disk capacitor thickness	0.25

where K_{11} denotes the elastic splay constant of the LC mixture (see Table 1).

During measurement, the upper plate was grounded through external bias tees (see Fig. 4), which provide also additional protection in case the inherent DC block of the phase shifter fails. The lower plate was connected to a 60 V DC power supply for biasing the LC (see Fig. 3 and Fig. 4, respectively).

Fig. 5 shows the scattering parameters. It can be seen that the matching is below −10 dB for a frequency range from 21 GHz to 27 GHz, which is slightly better than predicted by the simulation. This is caused by non-covered loss mechanisms, which also impact the insertion loss by roughly 2 dB. Depending on the tuning state, the measured insertion loss ranges from around 3.5 dB to 5.5 dB. The contribution of the coaxial transitions and the linear taper to the overall insertion loss is roughly 1 dB, which was estimated using a supplementary back to back assembly, revealing 0.5 dB and 1 dB of insertion loss in simulation and measurement, respectively. Despite of the 2 dB difference, the measured insertion loss conforms well to the simulated data up to 27 GHz, where the measurement shows a large drop. This stems from the used SMA thread-in connectors and accords to their specified frequency limit of 26.5 GHz. Here, higher order modes are excited despite the fundamental mode. The result is mode mismatch and signal loss as observed. With appropriate connectors for higher frequencies (e.g. K-connectors), the presented phase shifter should also be operable above 27 GHz as depicted by the simulation, since the simulation model does not include the connectors.

From the linear phase and flat group delay depicted in Fig. 6, it can be concluded that the phase shifter exhibits no dispersion as can be expected for a purely line based phase shifter.

$$\varepsilon = \varepsilon_0 \begin{bmatrix} \varepsilon_{\mathrm{r},\parallel}\sin^2(\alpha) + \varepsilon_{\mathrm{r},\perp}\cos^2(\alpha) & 0 & \frac{1}{2}\left(\varepsilon_{\mathrm{r},\parallel} - \varepsilon_{\mathrm{r},\perp}\right)\sin(2\alpha) \\ 0 & \varepsilon_{\mathrm{r},\perp} & 0 \\ \frac{1}{2}\left(\varepsilon_{\mathrm{r},\parallel} - \varepsilon_{\mathrm{r},\perp}\right)\sin(2\alpha) & 0 & \varepsilon_{\mathrm{r},\parallel}\cos^2(\alpha) + \varepsilon_{\mathrm{r},\perp}\sin^2(\alpha) \end{bmatrix} \tag{6}$$

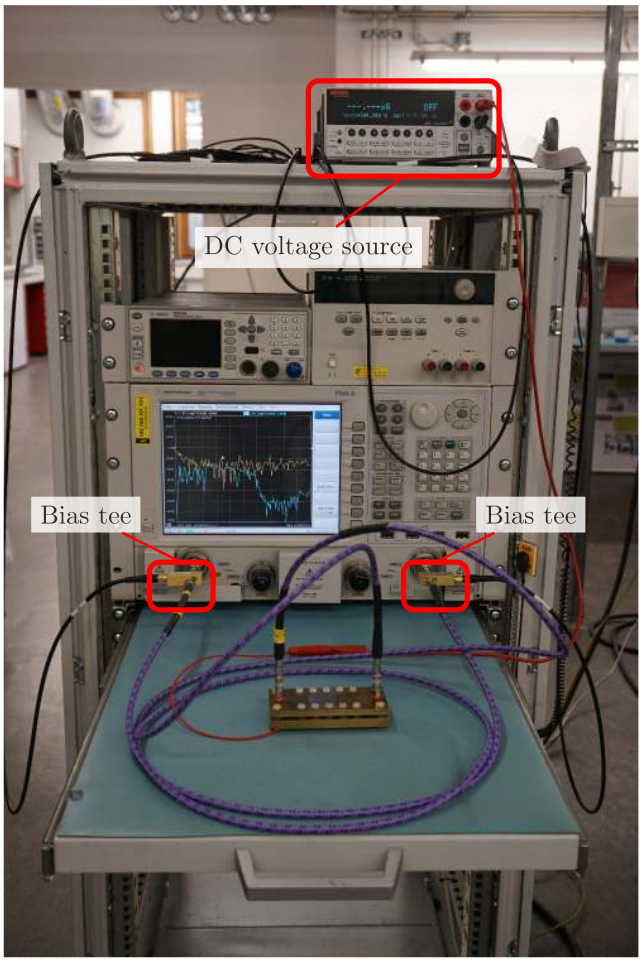

FIGURE 4. Measurement setup with DC voltage source (top), network analyzer with attached bias tees (middle) and RGW phase shifter (bottom) attached to the bias tees. The DC voltage is supplied by the red cable to the bottom plate of the phase shifter. The ground reference is supplied through the K-cables and the bias tees.

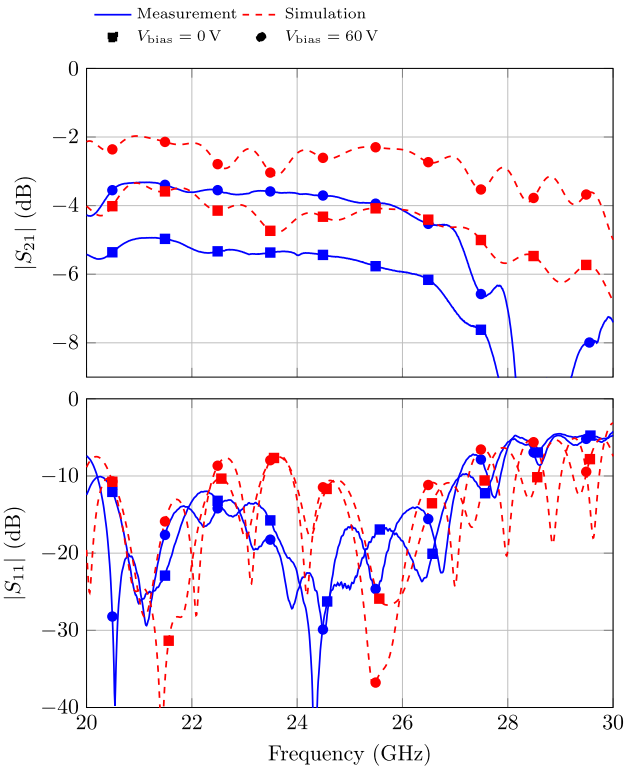

FIGURE 5. Measured and simulated scattering parameters of the RGW phase shifter.

To assess the aimed shielding property of the RGW, the E-field in the cross section of the plane centered in the LC layer was evaluated in simulation. With a perpendicular LC alignment, the worst case was assumed. The results are depicted for a frequency of $f = 25\,\text{GHz}$ in Fig. 8 for the three and two row RGW. Here, one can observe a field damping of 79 dB at a distance of $3\lambda_0$ from the waveguides center for the RGW with three bed of nails rows. The two row RGW exhibits only a slightly less damping of 76 dB, which justifies the choice for the implementation of the phase shifter. To compare these field damping results to common waveguides, the models of the Microstrip and Stripline depicted in Fig. 7 have been simulated and evaluated analogously (see Fig. 8). For both waveguides, different scenarios were simulated: A purely theoretic scenario with air as supporting superstrate material (i.e. the material above the actual waveguide's LC substrate), since the bed of nail section of the RGW is also mainly filled with air. For a more practical scenario, a common microwave substrate (Rogers RO4003C) has been assumed as superstrate. In both cases, the superstrate thickness has been altered between $d = 3.4\,\text{mm}$ for comparison to the RGW and $d = 0.5\,\text{mm}$ for a more practical use case and the corresponding line widths were adjusted to match the 14 Ω line impedance of the RGW phase shifter. Here, it can be observed that the implemented two row RGW suppresses the E-field at $3\lambda_0$ by additional 43 dB compared to a similar Microstrip setup and by additional 42 dB compared to a similar Stripline setup, both on the Rogers substrate. Assuming a thinner superstrate, the damping of the Microstrip setup increases but the suppression is still 18 dB larger for the two row RGW. Contrary, the damping of the Stripline setup decreases and exhibits a 58 dB less damping compared to the RGW. Only the theoretical scenarios of air filled waveguides show the least difference to the RGW with 8 dB fewer suppression, mainly caused by the lower dielectric constant of air, leading to a field displacement towards air.

This shielding property could also be confirmed during the measurements by moving a metallic perturber alongside the bed of nails structure, which had no influence on the measurement result.

A sweep over the bias voltage (see Fig. 9 and Fig. 10) revealed a saturation of the phase variation at around $V_{\text{bias}} = 60\,\text{V}$, indicating complete alignment of liquid crystal with the bias electric field. The maximum differential phase shift is shown in Fig. 9 by the red and blue curves for simulation and measurement, respectively. It takes roughly 7 s to achieve the parallel state. As already mentioned, there

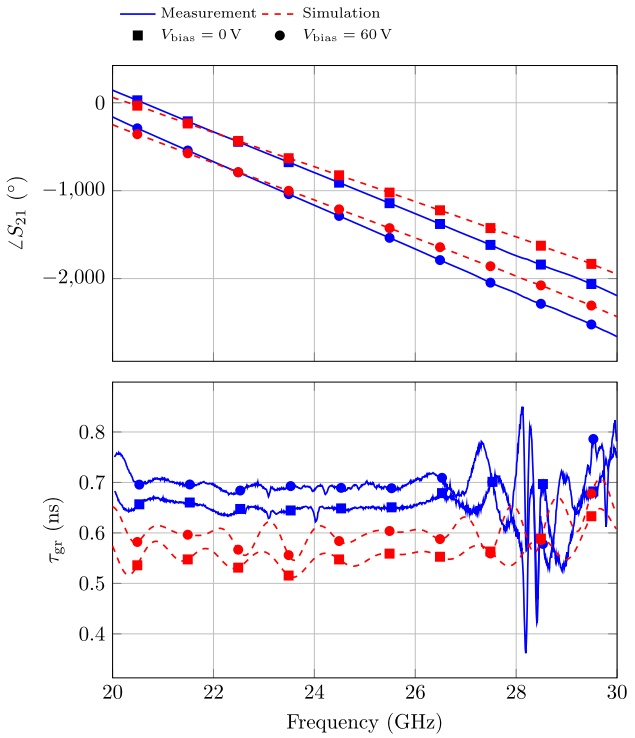

FIGURE 6. Measured and simulated phase and group delay of the RGW phase shifter.

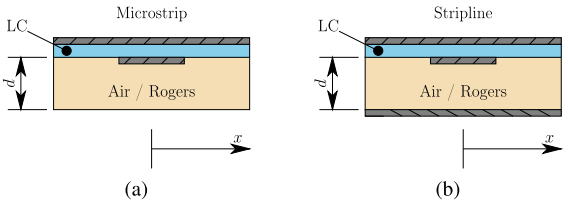

FIGURE 7. Schematic view of the simulation models used to compare the shielding properties of the RGW to Microstrip and Stripline, highlighting the varied parameter superstrate thickness d. For comparison, the corresponding line widths have been adjusted to match the 14 Ω line impedance of the RGW phase shifter.

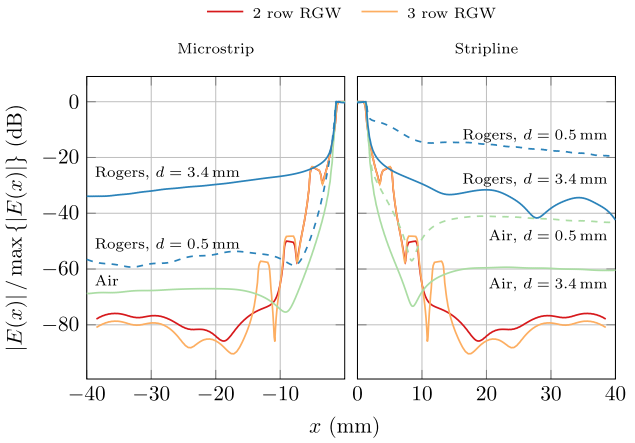

FIGURE 8. Simulated normalized E-field of Microstrip, Stripline and RGW, evaluated in the cross section of the plane centered in the LC layer of the corresponding waveguide at $f = 25$ GHz for perpendicular LC alignment.

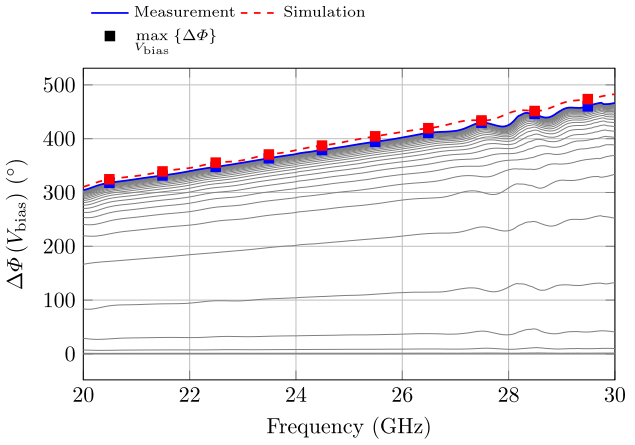

FIGURE 9. Measured and simulated differential phase shift of the RGW phase shifter in dependence of frequency. The colored curves depict the maximum phase shift in simulation and measurement, respectively. For clarity, the gray set of curves shows the voltage dependency only for the measurement data.

are only two electrodes and there is no active way of re-aligning the LC, hence the phase shifter needs more than 10 min to return to its unbiased state. Here, simulation and measurement show close agreement and the goal of at least 360° of differential phase shift is accomplished.

The FoM for the phase shifter as defined by (1) is shown in Fig. 11. Due to the 2 dB higher insertion loss in the measurement, the measured FoM is roughly 30 °/dB lower than predicted by the simulation, exhibiting a maximum of 70 °/dB at 25 GHz.

In the presented measurement, the phase shifter has been biased by a DC electric field. Despite the current necessary to load the capacitance between the top and bottom plate of the phase shifter, no additional power is required to bias the LC. However, in a practical application, the LC will be biased with a low frequency alternating current (AC) field of around $f_{bias} = 1$ kHz to prevent degradation of the LC mixture due to electrochemical effects. In this case, the capacitance formed by the phase shifter and the corresponding equivalent series resistance will affect the biasing power consumption. To assess these losses, a low frequency simulation was performed and the capacitance of the built phase shifter was measured. For the biasing scenario, a maximum bias with $V_{bias} = 60$ V (peak) was assumed. The simulated admittance is $Y = 138 \times 10^{-21}$ S + j516 nS which translates to a capacitance of $C = 82$ pF and an equivalent series resistance of ESR = 518 nΩ, leading to ohmic losses of $P = 248 \times 10^{-18}$ W and hence being practically negligible. The measured capacitance was almost twice the simulated with $C = 160$ pF due to the extended top and bottom plates for the mechanical fixation. The equivalent series resistance was not measurable. Table 3 summarizes the simulated and measured results including the reactive power and current,

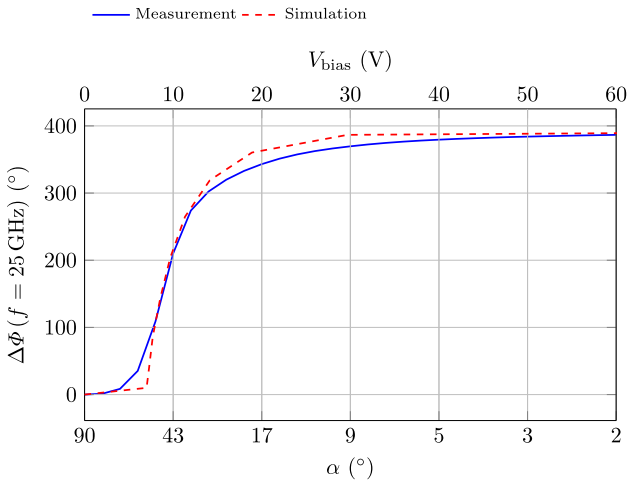

FIGURE 10. Measured and simulated differential phase shift of the RGW phase shifter in dependence of biasing voltage V_{bias} and director tilt angle α at $f = 25$ GHz.

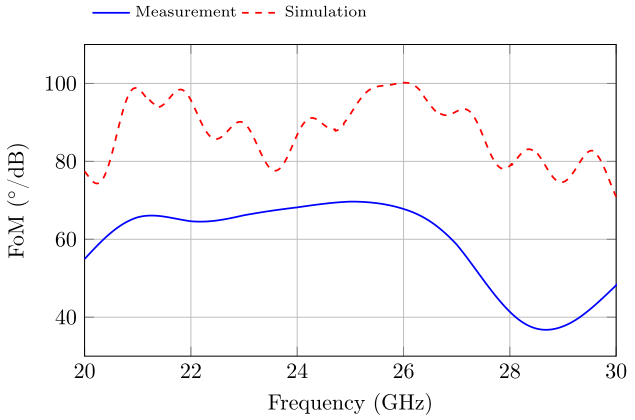

FIGURE 11. Measured and simulated FoM of the RGW phase shifter.

TABLE 3. Simulated and measured biasing capacitance of the RGW phase shifter and the corresponding loading current and apparent loss for a full biasing of $V_{\text{bias}} = 60$ V (peak) at $f_{\text{bias}} = 1$ kHz.

	C (pF)	I_{bias} (µA)	Q (µvar)
Simulation	82.1	30.9	928
Measurement	160	60.3	1810

which has to be provided to the phase shifter for full bias. For the built phase shifter a loading current of $I_{\text{bias}} = 60.3\ \mu$A and hence a reactive power of $Q = 1.81$ mvar needs to be provided for full phase shift.

IV. CONCLUSION

This paper examines the applicability of gap waveguides for LC-based electrically-tunable phase shifters. For this purpose, a proof of concept demonstrator was implemented operating around 26 GHz. Hereby, the gap waveguide's inherent property of DC decoupling is utilized to form the electrodes for LC biasing directly from the waveguide surroundings, eliminating the need for a specific electrode design. A ridge was introduced to further reduce the LC cavity height to 0.2 mm. The capacitive coaxial coupling of this ridge gap waveguide additionally acts as DC block for the RF feed, eliminating the need for external bias tees. To the author's best knowledge, this is the first time that such a device was implemented.

TABLE 4. Comparison of different LC based phase shifters according to their FoM and size.

Type	f_{op} GHz	$\Delta\Phi(f_{\text{op}})$ °	Gain dB	FoM (f_{op}) °/dB	Volume mm^3	Ref.
HWG*	35	110	−0.55	200	758.7	[8]
HWG	35	110	xxx	150	758.7	[8]
SW Fiber	102.5	825	n/a	145	121.5	[18]
IMSL#	24	n/a	n/a	110	n/a	[17]
Ridged HWG	108	600	−8	78	54.8	[16]
HWG*	105	120	−2 to −1.5	70	41.9	[19]
RGW	25	387	−5.5 to −3.5	70	7424.0	This Work
CPW#	79	408	−6.15 to −4.56	66	144.9	[20]
Loaded TLines#	76	92	−2.2	42	240×10^{-5}	[21]
IMSL#	20	270	n/a	40	1434.0	[22]
IMSL# on NaM	60	89	−2.4	37	0.5	[23]
SSPP*#	10	76	−5 to −3	23	2584.8	[24]
HWG*	45	280	−13.5	21	576.0	[25]
Loaded TLines#	61	243	−12	20	75.4	[26]
MS and RTPS#	59.5	188.5	−11	17	1.7	[27]
IMSL#	34	249	−16 to −8	16	134.6	[28]
CPW#	35	100	−7 to −1	14	1.8	[29]
RTPS#	61	170	−14	12	15.9	[26]
RTPS#	61	130	n/a	11	10.2	[30]
Stripline in LTCC#	30	60	−6	10	97.5	[31]

*	magnetic biasing	#	planar
HWG	Hollow waveguide	NaM	Nanowire membrane
SW Fiber	Subwavelength fiber	SSPP	Spoof surface plasmon polaritons
IMSL	Inverted Microstrip line	MS	Microstrip
RGW	Ridge gap waveguide	RTPS	Reflection type phase shifter
CPW	Coplanar waveguide	LTCC	Low temperature cofired ceramics

The measurement of this demonstrator revealed a differential phase shift of 387° at 25 GHz, with an insertion loss ranging from 3.5 dB to 5.5 dB depending on the tuning state. Here, the maximum FoM achieved is 70 °/dB (see (1)), which is comparable to other similar phase shifter topologies like ridged hollow waveguide [16] or inverted Microstrip lines [17], but cannot compete with hollow waveguide [8] or sub wavelength fiber [18] topology. A more comprehensive comparison with other LC based phase shifters is given in Table 4. Fig. 12 further condenses the data from Table 4 by comparing the achieved FoM versus the electrical size of the phase shifters. Here, it is apparent that, although achieving a reasonable FoM, the realized RGW phase shifter is still quite bulky.

Apart from its size, the proof of concept here presents the promising potential of gap waveguides for packaging LC in tunable microwave components. The inherent DC decoupling eases the biasing network and electrode design. Attenuating the E-field by 76 dB, the bed of nail structure not only prevents the excitation of parallel plate modes, but also shields the RGW laterally without the need for via placing in the LC layer. Further, the top and bottom metal layer act as RF ground, shielding the device also in a multilayer setup and making integration easier.

The loading current and necessary reactive power to fully bias the presented phase shifter was assessed to $I_{\text{bias}} = 60.3\ \mu$A and $Q = 1.81$ mvar, respectively. This comparatively small current might sum up in the application

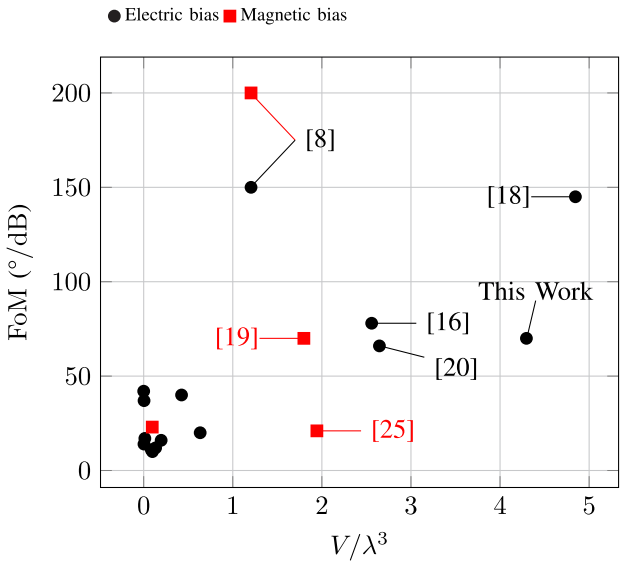

FIGURE 12. FoM versus electrical size for different LC based phase shifters and the presented RGW phase shifter.

specific biasing network (e.g. phased array) and might create additional power loss there.

The size could be addressed by implementing the gap waveguide in planar, mushroom-structure like PCB topologies [32] or by micromachining technologies [33], being especially interesting for millimeter wave frequencies. Further size reduction could be achieved, using resonant structures instead of a pure line based phase shifter, leaving scope for further investigations.

ACKNOWLEDGEMENTS

The authors would like to thank Merck KGaA for providing the LC.

REFERENCES

[1] K.-J. Koh and G. M. Rebeiz, "0.13-μm CMOS phase shifters for X-, Ku-, and K-band phased arrays," *IEEE J. Solid-State Circuits*, vol. 42, no. 11, pp. 2535–2546, Nov. 2007.

[2] S. I. M. Sheikh, A. A. P. Gibson, M. Basorrah, G. Alhulwah, K. Alanizi, M. Alfarsi, and J. Zafar, "Analog/Digital ferrite phase shifter for phased array antennas," *IEEE Antennas Wireless Propag. Lett.*, vol. 9, pp. 319–321, 2010.

[3] J. J. P. Venter, T. Stander, and P. Ferrari, "*X*-band reflection-type phase shifters using coupled-line couplers on single-layer RF PCB," *IEEE Microw. Wireless Compon. Lett.*, vol. 28, no. 9, pp. 807–809, Sep. 2018.

[4] C.-C. Chang, Y.-C. Chen, and S.-C. Hsieh, "A V-Band three-state phase shifter in CMOS-MEMS technology," *IEEE Microw. Wireless Compon. Lett.*, vol. 23, no. 5, pp. 264–266, May 2013.

[5] C. Weickhmann, R. Jakoby, E. Constable, and R. A. Lewis, "Time-domain spectroscopy of novel nematic liquid crystals in the terahertz range," in *Proc. 38th Int. Conf. Infr., Millim., Terahertz Waves (IRMMW-THz)*, Sep. 2013, pp. 1–2.

[6] P. G. de Gennes and J. Prost, *The Physics of Liquid Crystals*, 2nd ed. New York, NY, USA: Oxford Univ. Press, 1993.

[7] S. Muller, P. Scheele, C. Weil, M. Wittek, C. Hock, and R. Jakoby, "Tunable passive phase shifter for microwave applications using highly anisotropic liquid crystals," in *IEEE MTT-S Int. Microw. Symp. Dig.*, Jun. 2004, pp. 1153–1156.

[8] A. Gaebler, F. Goelden, A. Manabe, M. Goebel, S. Mueller, and R. Jakoby, "Investigation of high performance transmission line phase shifters based on liquid crystal," in *Proc. Eur. Microw. Conf. (EuMC)*, Sep. 2009, pp. 594–597.

[9] C. Weickhmann, N. Nathrath, R. Gehring, A. Gaebler, M. Jost, and R. Jakoby, "A light-weight tunable liquid crystal phase shifter for an efficient phased array antenna," in *Proc. Eur. Microw. Conf.*, Oct. 2013, pp. 428–431.

[10] P.-S. Kildal, E. Alfonso, A. Valero-Nogueira, and E. Rajo-Iglesias, "Local metamaterial-based waveguides in gaps between parallel metal plates," *IEEE Antennas Wireless Propag. Lett.*, vol. 8, pp. 84–87, 2009.

[11] A. Jimenez Saez, A. Valero-Nogueira, J. I. Herranz, and B. Bernardo, "Single-layer cavity-backed slot array fed by groove gap waveguide," *IEEE Antennas Wireless Propag. Lett.*, vol. 15, pp. 1402–1405, 2016.

[12] A. Vosoogh, A. Haddadi, A. U. Zaman, J. Yang, H. Zirath, and A. A. Kishk, "*W*-band low-profile monopulse slot array antenna based on gap waveguide corporate-feed network," *IEEE Trans. Antennas Propag.*, vol. 66, no. 12, pp. 6997–7009, Dec. 2018.

[13] M. Ferrando-Rocher, J. I. Herranz-Herruzo, A. Valero-Nogueira, B. Bernardo-Clemente, A. U. Zaman, and J. Yang, "8 ×8 ka-band dual-polarized array antenna based on gap waveguide technology," *IEEE Trans. Antennas Propag.*, vol. 67, no. 7, pp. 4579–4588, Jul. 2019.

[14] M. Baquero-Escudero, A. Valero-Nogueira, M. Ferrando-Rocher, B. Bernardo-Clemente, and V. E. Boria-Esbert, "Compact combline filter embedded in a bed of nails," *IEEE Trans. Microw. Theory Techn.*, vol. 67, no. 4, pp. 1461–1471, Apr. 2019.

[15] F. Gölden, "Liquid crystal based microwave components with fast response times: Material, technology, power handling capability," Ph.D. dissertation, Dept. Elect. Eng., Technische Univ. Darmstadt, Darmstadt, Germany, Jun. 2010. [Online]. Available: http://tuprints.ulb.tu-darmstadt.de/2203/

[16] S. Mueller, F. Goelden, P. Scheele, M. Wittek, C. Hock, and R. Jakoby, "Passive phase shifter for W-Band applications using liquid crystals," in *Proc. Eur. Microw. Conf.*, Sep. 2006, pp. 306–309.

[17] C. Weil, S. Muíller, P. Scheele, P. Best, G. Luíssem, and R. Jakoby, "Highly-anisotropic liquid-crystal mixtures for tunable microwave devices," *Electron. Lett.*, vol. 39, no. 24, pp. 1732–1734, 2003.

[18] R. Reese, E. Polat, H. Tesmer, J. Strobl, C. Schuster, M. Nickel, A. B. Granja, R. Jakoby, and H. Maune, "Liquid crystal based dielectric waveguide phase shifters for phased arrays at W-Band," *IEEE Access*, vol. 7, pp. 127032–127041, 2019.

[19] M. Jost, R. Reese, M. Nickel, S. Schmidt, H. Maune, and R. Jakoby, "Interference based W-band single-pole double-throw with tunable liquid crystal based waveguide phase shifters," in *IEEE MTT-S Int. Microw. Symp. Dig.*, Jun. 2017, pp. 184–187.

[20] J. F. Li, H. Xu, and D. P. Chu, "Design of liquid crystal based coplanar waveguide tunable phase shifter with no floating electrodes for 60–90 GHz applications," in *Proc. 46th Eur. Microw. Conf. (EuMC)*, Oct. 2016, pp. 1047–1050.

[21] C. Fritzsch, F. Giacomozzi, O. H. Karabey, S. Bildik, S. Colpo, and R. Jakoby, "Advanced characterization of a W-band phase shifter based on liquid crystals and MEMS technology," *Int. J. Microw. Wireless Technol.*, vol. 4, no. 3, pp. 379–386, Jun. 2012.

[22] L. Cai, H. Xu, J. Li, and D. Chu, "High fom liquid crystal based microstrip phase shifter for phased array antennas," in *Proc. Int. Symp. Antennas Propag. (ISAP)*, Oct. 2016, pp. 402–403.

[23] M. Jost, J. S. K. Gautam, L. G. Gomes, R. Reese, E. Polat, M. Nickel, J. M. Pinheiro, A. L. C. Serrano, H. Maune, G. P. Rehder, P. Ferrari, and R. Jakoby, "Miniaturized liquid crystal slow wave phase shifter based on nanowire filled membranes," *IEEE Microw. Wireless Compon. Lett.*, vol. 28, no. 8, pp. 681–683, Aug. 2018.

[24] C. Ding, F.-Y. Meng, J.-Q. Han, H.-L. Mu, Q.-Y. Fang, and Q. Wu, "Design of filtering tunable liquid crystal phase shifter based on spoof surface plasmon polaritons in PCB technology," *IEEE Trans. Compon., Packag., Manuf. Technol.*, vol. 9, no. 12, pp. 2418–2426, Dec. 2019.

[25] T. Nose, T. Ito, R. Ito, and M. Honma, "Basic performance of rectangular waveguide type liquid crystal phase shifter driven by magnetic field," in *Proc. 43rd Int. Conf. Infr., Millim., THz Waves (IRMMW-THz)*, Sep. 2018, pp. 1–2.

[26] S. Bulja, D. Mirshekar-Syahkal, M. Yazdanpanahi, R. James, S. E. Day, and F. A. Fernánd, "Liquid crystal based phase shifters in 60 GHz band," in *Proc. 3rd Eur. Wireless Technol. Conf.*, Sep. 2010, pp. 37–40.

[27] P. Deo, D. Mirshekar-Syahkal, L. Seddon, S. E. Day, and F. A. Fernandez, "Beam steering 60 GHz slot antenna array using liquid crystal phase shifter," in *Proc. 8th Eur. Conf. Antennas Propag. (EuCAP)*, Apr. 2014, pp. 1005–1007.

[28] C. D. Woehrle, D. T. Doyle, S. A. Lane, and C. G. Christodoulou, "Space radiation environment testing of liquid crystal phase shifter devices," *IEEE Antennas Wireless Propag. Lett.*, vol. 15, pp. 1923–1926, 2016.

[29] F. Sahbani, N. Tentillier, A. Gharsallah, A. Gharbi, and C. Legrand, "New tunable coplanar microwave phase shifter with nematic crystal liquid," in *Proc. 3rd Int. Design Test Workshop*, Dec. 2008, pp. 78–81.

[30] S. Bulja, D. Mirshekar-Syahkal, M. Yazdanpanahi, R. James, S. E. Day, and F. A. Fernandez, "60 GHz reflection type phase shifter based on liquid crystal," in *Proc. IEEE Radio Wireless Symp. (RWS)*, Jan. 2010, pp. 697–699.

[31] M. Jost, S. Strunck, A. Heunisch, A. Wiens, A. E. Prasetiadi, C. Weickhmann, B. Schulz, M. Quibeldey, O. H. Karabey, T. Rabe, R. Follmann, D. Koether, and R. Jakoby, "Continuously tuneable liquid crystal based stripline phase shifter realised in LTCC technology," in *Proc. 10th Eur. Microw. Integr. Circuits Conf. (EuMIC)*, Sep. 2015, pp. 1260–1263.

[32] E. Pucci, E. Rajo-Iglesias, and P.-S. Kildal, "New microstrip gap waveguide on mushroom-type EBG for packaging of microwave components," *IEEE Microw. Wireless Compon. Lett.*, vol. 22, no. 3, pp. 129–131, Mar. 2012.

[33] S. Farjana, S. Rahiminejad, A. U. Zaman, J. Hansson, M. A. Ghaderi, S. Haasl, and P. Enoksson, "Polymer based 140 GHz planar gap waveguide array antenna for line of sight (LOS) MIMO backhaul links," in *IEEE MTT-S Int. Microw. Symp. Dig.*, Jul. 2019, pp. 148–150.

MATTHIAS NICKEL (Graduate Student Member, IEEE) was born in Wetzlar, Germany, in 1987. He received the master's degree from Technische Universität Darmstadt, Darmstadt, Germany, in 2014. Since 2014, he has been with the Institute of Microwave Engineering and Photonics, Technische Universität Darmstadt. His current research interests include active phased array antennas and liquid crystal-based microwave components for millimeter-wave systems.

ALEJANDRO JIMÉNEZ-SÁEZ (Student Member, IEEE) was born in Valencia, Spain, in 1992. He received the master's degree in telecommunications engineer from the Polytechnic University of Valencia and the master's degree in electrical engineering from the Technische Universität Darmstadt, Germany, in 2017, where he is currently pursuing the Ph.D. degree with the Institute of Microwave Engineering and Photonics. His current research interests include passive chipless RFID, high-Q resonators, and electro-magnetic bandgap structures in microwave and millimeter-wave frequencies.

PRANNOY AGRAWAL (Graduate Student Member, IEEE) was born in Delhi, India, in 1991. He received the bachelor's degree from GGSIP University, Delhi, India, in 2012, and the master's degree from Technische Universität Darmstadt, Darmstadt, Germany, in 2018. Since 2018, he has been with the Institute of Microwave Engineering and Photonics, Technische Universität Darmstadt. His current research interests include tunability and acoustic modeling of barium strontium titanate (BST) composites and high-power varactors.

AHMED GADALLAH (Member, IEEE) received the bachelor's degree in electronic engineering from the Faculty of Electronic Engineering, Menofia University, Menofia, Egypt, in 2010, and the master's degree in electronics and communications Engineering from the Egypt Japan University of Science and Technology (EJUST), Alexandria, Egypt, in 2015. From 2011 to 2013, he was a Teaching Assistant with the Aswan Faculty of Engineering, Aswan University, Egypt. From 2015 to 2017, he was a Research Assistant with EJUST, where his research was focused on high efficiency power amplifiers. Since March 2017, he has been a Research Scientist with the Circuit Design Department, Innovations for High Performance Microelectronics (IHP), Frankfurt (Oder), Germany. His current research interest includes RF and mm-wave circuit design.

ANDREA MALIGNAGGI received the B.Sc. and M.Sc. degrees in microelectronics from the University of Catania, Catania, Italy, in 2005 and 2008, respectively, the M.A.S. degree in embedded systems design from the ALaRI Institute, University of Lugano, Lugano, Switzerland, in 2010, and the Ph.D. degree from the Berlin Institute of Technology, Berlin, Germany, in 2016, concerning the design of CMOS 60 GHz circuits. Since 2015, he has been with the IHP Leibniz institute, Frankfurt (Oder), Germany. His current research interests include design and optimization of high-frequency circuits and systems.

CHRISTIAN SCHUSTER (Student Member, IEEE) was born in Wiesbaden, Germany, in 1988. He received the B.Sc. and M.Sc. degrees from Technische Universität Darmstadt, Darmstadt, Germany, in 2012 and 2015, respectively. He is currently pursuing the Ph.D. degree with the Microwave Engineering Group, Technische Universität Darmstadt. His research interests include tunable microwave filters and reconfigurable RF transceiver systems.

ROLAND REESE (Graduate Student Member, IEEE) was born in Darmstadt, Germany, in 1990. He received the B.Sc. and M.Sc. degrees in electrical engineering from Technische Universität Darmstadt, in 2013 and 2015, respectively, where he is currently pursuing the Ph.D. degree with the Institute for Microwave Engineering and Photonics with a focus on new devices and antennas in the millimeter wave range.

HENNING TESMER (Graduate Student Member, IEEE) was born in Kassel, Germany, in 1992. He received the B.Sc. and M.Sc. degrees from Technische Universität Darmstadt, Darmstadt, Germany, in 2015 and 2018, respectively, where he is currently pursuing the Ph.D. degree with the Institute of Microwave Engineering and Photonics. His current research interests include liquid crystal-based tunable dielectric waveguides and components for millimeter-wave applications.

ERSIN POLAT (Student Member, IEEE) was born in Alzenau, Germany, in 1991. He received the B.Sc. and M.Sc. degrees from Technische Universität Darmstadt, Darmstadt, Germany, in 2014 and 2017, respectively, where he is currently pursuing the Ph.D. degree with the Microwave Engineering Group. His current research interests include tunable microwave filters and material characterization.

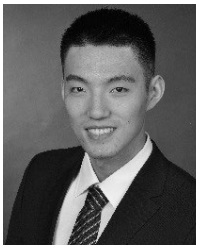

DONGWEI WANG was born in Taiyuan, Shanxi, China, in 1991. He received the B.Eng. degree from Zhejiang University, Hangzhou, Zhejiang, China, and the M.Sc. degree from Karlsruher Institut für Technologie, Karlsruhe, Germany. He is currently pursuing the Ph.D. degree with the Institute of Microwave Engineering and Photonics, Technische Universität Darmstadt, Darmstadt, Germany. His current research interest includes liquid crystal-based tunable planar devices with slow-wave effect.

PETER SCHUMACHER (Graduate Student Member, IEEE) was born in Wiesbaden, Germany, in 1990. He received the B.Sc. and M.Sc. degrees in electrical engineering and information technology from Technische Universität Darmstadt, Darmstadt, Germany, in 2017 and 2018, respectively, where he is currently pursuing the Ph.D. degree with the Institute of Microwave Engineering and Photonics. His current research interests include transparent glass ceramics antenna arrays and liquid crystal-based microwave components for millimeter wave applications.

ROLF JAKOBY (Member, IEEE) was born in Kinheim, Germany, in 1958. He received the Dipl.Ing. degrees in electrical engineering from the University of Siegen, Germany, in 1985 and 1990, respectively. In January 1991, he joined the Research Center of Deutsche Telekom, Darmstadt, Germany. Since April 1997, he has been a Full professorship with TU Darmstadt, Germany. He is a co-inventor of nine patents and participates on 11 awards in the last six years. His research interests include RFID, micro- and millimeter wave detectors and sensors for various applications, and in particular on reconfigurable RF passive devices by using novel approaches with metamaterial structures, liquid crystal, and ferroelectric thick/thin film technologies. He is a member of the Society for Information Technology (ITG) of the VDE and the IEEE societies MTT and AP. He is an organizer of various workshops and a member of various TPCs. He has been Chairman of the European Microwave Conference 2007 and the German Microwave Conference 2011. He is the Editor-in-Chief of FREQUENZ. In 1992, he received an Award from the CCI Siegen and in 1997, the ITG-Prize for an excellent publication in the IEEE TRANSACTIONS ON ANTENNAS AND PROPAGATION.

DIETMAR KISSINGER (Senior Member, IEEE) received the Dipl.Ing., Dr.Ing. and Habilitation degrees in electrical engineering from FAU Erlangen-Nürnberg, Germany, in 2007, 2011, and 2014, respectively. From 2007 to 2010, he was with Danube Integrated Circuit Engineering, Linz, Austria, where he worked as a System and Application Engineer with the Automotive Radar Group. From 2010 to 2014, he held a position as a Lecturer and the Head of the Radio Frequency Integrated Sensors Group, Institute for Electronics Engineering, Erlangen. From 2015 to 2018, he was with Technische Universität Berlin and the Head of the Circuit Design Department, IHP, Frankfurt (Oder). Since 2019, he has been a Full Professor of high-frequency circuit design with Ulm University and the Head of the Institute of Electronic Devices and Circuits. His current research interests include silicon high-frequency and high-speed integrated circuits and systems for communication and automotive, industrial, security and biomedical sensing applications. He has authored or coauthored over 300 technical articles He holds several patents. He is a member of the European Microwave Association (EuMA), the German Information Technology Society (ITG), and the Society of Microelectronics, Microsystems and Precision Engineering (VDE/VDI GMM). He currently serves as a member of the technical program committee of the International Microwave Symposium (IMS), European Solid-State Circuits Conference (ESSCIRC), and the European Microwave Week (EuMW) and the TPC Chair of the 2021 German Microwave Conference (GeMiC). He received the 2017 IEEE MTT-S Outstanding Young Engineer Award, the 2017 VDE/VDI GMM-Prize, and the 2018 VDE ITG-Prize. He was the co-recipient of more than ten best paper awards. He was a two-time Chair of the IEEE Topical Conference on Wireless Sensors and Sensor Networks (WiSNet) and a two-time Chair of the IEEE Topical Conference on Biomedical Wireless Technologies, Networks and Sensing Systems (BioWireless). He further served as a member of the 2013 and 2017 European Microwave Week (EuMW) Organizing Committee and the 2018 IEEE MTT-S International Microwave Symposium (IMS) Steering Committee, and as the Executive Committee Chair of the Radio and Wireless Week (RWW). He was a nine-time Guest Editor for the *IEEE Microwave Magazine*. He has served as an Associate Editor for the IEEE TRANSACTIONS ON MICROWAVE THEORY AND TECHNIQUES. He was the Chair of the IEEE MTT-S Technical Committee on Microwave and Millimeter-Wave Integrated Circuits (MTT-14). He is currently an Elected Member of the IEEE MTT-S Administrative Committee.

HOLGER MAUNE (Senior Member, IEEE) was born in Cologne, Germany, in 1981. He received the Dipl.Ing. degree in communications engineering from Technische Universitaet Darmstadt, Darmstadt, Germany, in 2006 and 2011, respectively. His research interests include reconfigurable smart radio frequency (RF) systems based on electronically tunable microwave components, such as phase shifters, adaptive matching networks, tunable filters, duplexer, and multiband antennas. Their integration into system components such as adaptively matched power amplifiers, reconfigurable RF frontends or fully integrated electronically beam-steering transceiver antenna arrays is in the focus of the work.